Möbius-invariant surface energies and ridges

By Shin Yoshizawa[1] AND Alexander Belyaev[2]

[1]Image Processing Research Team, RIKEN, Japan, shin@riken.jp

[2]Institute of Sensors, Signals & Systems, Heriot-Watt University, UK, a.belyaev@hw.ac.uk

Abstract

In this paper, we study Möbius-invariant curvature-based surface energies and characteristic surface curves. We demonstrate how Möbius-invariant curvature-based surface energies can be used to achieve a better detection of salient surface creases.

1. Introduction

Invariance is a foundational concept in physical theories and mathematical constructions. Invariance serves as a central pillar for pattern recognition and is of fundamental importance for computer vision and geometric modeling applications.

In this paper, we deal with curvature-based surface energies, surface curves, and parameters which are invariant under Möbius transformations. The Lie group of Möbius transformations is generated by inversions in spheres and, in addition to the sphere inversions, includes the translations, rotations, and similarity transformations (homotheties). High importance of Möbius transformations and invariants is justified by Liouvilles theorem on conformal mappings which states that any smooth conformal mapping on a domain of $\mathbb{R}^d$, $d \geq 3$ is a Möbius transformation (see, for example, (Blair 2000)). Figure 1 demonstrates an inversion of a complex mesh model. Curvature-based energies are widely used in mathematical, physical, engineering, and biological studies. Various invariance properties of curvature-based energies make them useful computer vision and geometric modeling applications.

In this study, we consider Möbius invariant curvature-based surface energies and use them for a robust detection of salient surface creases. All numerical experiments presented in this paper are performed on surfaces approximated by dense triangle meshes where their differential quantities are approximated by using the approach developed in (Yoshizawa et al. 2008).

2. Möbius cross energy of a link

Consider a pair of curves γ_1 and γ_2 in Euclidean three-space E^3 as illustrated in Fig. 2 (a). Let the curves be parameterized by their arc-lengths $s_1 \in I_1$ and $s_2 \in I_2$, respectively. The *Möbius cross energy* of the pair is defined by

$$E(\gamma_1, \gamma_2) = \iint\limits_{I_1 \times I_2} \frac{ds_1 ds_2}{|\gamma_1 - \gamma_2|^2}. \tag{2.1}$$

It is easy to show that this energy is Möbius invariant (Freedman et al. 1994; He 2002). Indeed let π be an inversion w.r.t a sphere of radius c centered at the origin of coordinates O. Let $\tilde{\boldsymbol{x}}$ and $\tilde{\boldsymbol{y}}$ be the inversion images of $\boldsymbol{x}$ and $\boldsymbol{y}$, respectively, as seen in Fig. 2 (b). Then $|\boldsymbol{x}|/|\tilde{\boldsymbol{y}}| = |\boldsymbol{y}|/|\tilde{\boldsymbol{x}}|$ and, therefore, the triangles $O\boldsymbol{x}\boldsymbol{y}$ and $O\tilde{\boldsymbol{y}}\tilde{\boldsymbol{x}}$ are similar. Thus

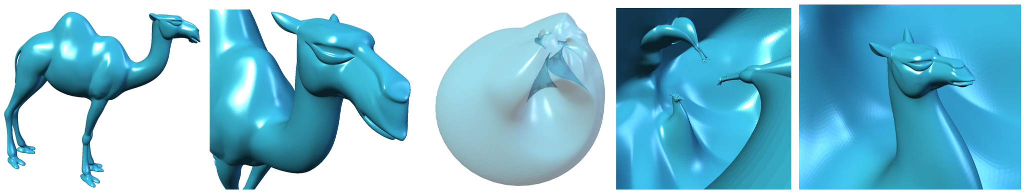

(a) (b) (c) (d) (e)

FIGURE 1. Inversion examples. (a,b): Input mesh. (c,d,e): Inversion of (a,b).

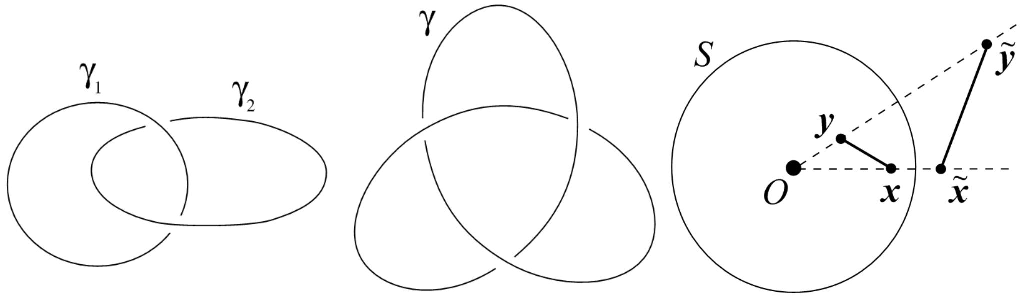

(a) (b)

FIGURE 2. Links, knots, and inversions. (a): a link and a knot. (b): an inversion w.r.t. sphere S.

$$\frac{|\boldsymbol{x}|}{|\boldsymbol{x}-\boldsymbol{y}|}=\frac{|\tilde{\boldsymbol{y}}|}{|\tilde{\boldsymbol{x}}-\tilde{\boldsymbol{y}}|},\qquad \frac{|\boldsymbol{y}|}{|\boldsymbol{x}-\boldsymbol{y}|}=\frac{|\tilde{\boldsymbol{x}}|}{|\tilde{\boldsymbol{x}}-\tilde{\boldsymbol{y}}|},\qquad \text{and}\qquad \frac{|\boldsymbol{x}||\boldsymbol{y}|}{|\boldsymbol{x}-\boldsymbol{y}|^2}=\frac{|\tilde{\boldsymbol{x}}||\tilde{\boldsymbol{y}}|}{|\tilde{\boldsymbol{x}}-\tilde{\boldsymbol{y}}|^2}.$$

It remains to note that

$$|d\tilde{\boldsymbol{x}}|=\frac{c^2}{|\boldsymbol{x}|^2}|d\boldsymbol{x}|=\frac{|\boldsymbol{x}||\tilde{\boldsymbol{x}}|}{|\boldsymbol{x}|^2}|d\boldsymbol{x}|=\frac{|\tilde{\boldsymbol{x}}|}{|\boldsymbol{x}|}|d\boldsymbol{x}|,\qquad |d\tilde{\boldsymbol{y}}|=\frac{|\tilde{\boldsymbol{y}}|}{|\boldsymbol{y}|}|d\boldsymbol{y}|,$$

and therefore,

$$\frac{|d\boldsymbol{x}||d\boldsymbol{y}|}{|\boldsymbol{x}-\boldsymbol{y}|^2}=\frac{|d\tilde{\boldsymbol{x}}||d\tilde{\boldsymbol{y}}|}{|\tilde{\boldsymbol{x}}-\tilde{\boldsymbol{y}}|^2}. \tag{2.2}$$

Möbius cross energy $E(\gamma_1,\gamma_2)$ defined by (2.1) is finite for a link but becomes infinite for a knot. So various generalizations of $E(\gamma,\gamma)$ are considered for knot analysis and visualization purposes (O'Hara 2003).

3. Möbius energies of a surface

Consider a smooth surface M and a point $\boldsymbol{x}$ on it. Let s_1 and s_2 be the curvature line arc-lengths corresponding to the curvature radii $R_1=1/k_1$ and $R_2=1/k_2$, where k_1 and k_2 are the principal curvatures ($k_1\geq k_2$) of M at $\boldsymbol{x}$. Denote by f_1 the arc-length of the curve on the R_1-focal surface corresponding to k_1-curvature line on M and by f_2 the arc-length of the curve on the R_2-focal surface corresponding to k_2-curvature line on M, see Figs 3 and 4.

According to (2.2) measure

$$\frac{df_1df_2}{(R_1-R_2)^2} \tag{3.1}$$

is Möbius invariant. It is not difficult to show that (Weatherburn 1927, Art. 75)

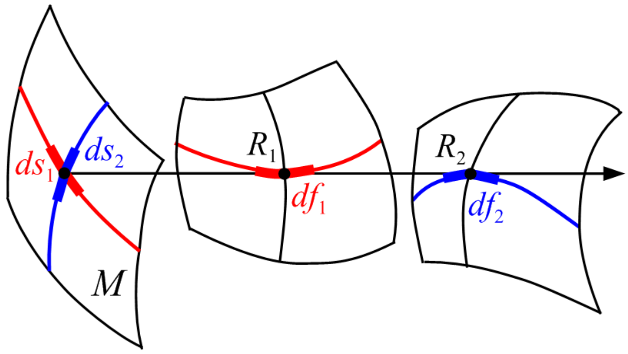

FIGURE 3. Surface M and its two corresponding focal surfaces.

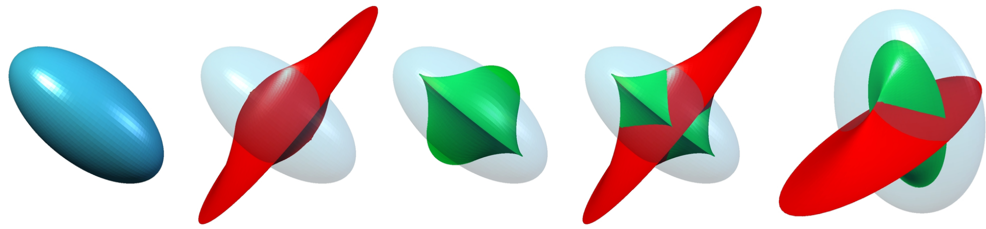

FIGURE 4. Focal surface examples. (a): Input ellipsoid mesh. (b): R_1-focal surface of (a). (c): R_2-focal surface of (a). (d,e): Both focal surfaces of (a).

$$df_1 = |\partial R_1/\partial s_1| ds_1 \qquad \text{and} \qquad df_2 = |\partial R_2/\partial s_2| ds_2. \tag{3.2}$$

Denote by $e_1 = \partial k_1/\partial s_1$ and $e_2 = \partial k_2/\partial s_2$ the derivatives of the principal curvatures k_1 and k_2 along their corresponding curvature lines, respectively. Now (3.1), (3.2), and relation $ds_1 ds_2 = dA$ imply that

$$\frac{|e_1||e_2|dA}{(k_1 - k_2)^2} \tag{3.3}$$

is Möbius invariant. Further, since (3.1) is invariant w.r.t. normal shifts, the same is true for (3.3).

Now we provide the reader with a more traditional derivation of the Möbius invariance of (3.1) and (3.3). Consider a smooth oriented surface M in E^3. Let π be an inversion w.r.t a sphere of radius $c > 0$ centered at the origin of coordinates. Denote by $\boldsymbol{x}$ and $\tilde{\boldsymbol{x}}$ the position vectors of M and the inverse surface $\tilde{M} = \pi(M)$, respectively. Then we have

$$\tilde{\boldsymbol{x}} = \frac{c^2}{r^2}\boldsymbol{x}, \qquad d\tilde{\boldsymbol{x}} = \frac{c^2}{r^2}d\boldsymbol{x} - 2\frac{c^2}{r^3}dr\,\boldsymbol{x}, \qquad d\tilde{\boldsymbol{x}}^2 = \frac{c^4}{r^4}d\boldsymbol{x}^2, \qquad \text{where} \qquad r = |\boldsymbol{x}|.$$

It is not difficult to show that

$$\tilde{k}_1 = -\frac{r^2}{c^2}k_2 - 2\frac{(\boldsymbol{x}\cdot\boldsymbol{n})}{c^2} \qquad \text{and} \qquad \tilde{k}_2 = -\frac{r^2}{c^2}k_1 - 2\frac{(\boldsymbol{x}\cdot\boldsymbol{n})}{c^2} \tag{3.4}$$

where $\boldsymbol{n}$ is the unit normal vector of $\boldsymbol{x}$, $\tilde{k}_1$ and $\tilde{k}_2$ are the principal curvatures ($\tilde{k}_1 \geq \tilde{k}_2$) of $\tilde{M}$ at $\tilde{\boldsymbol{x}}$, see (Weatherburn 1927, Art. 82-83) or Appendix A for derivations of (3.4). Thus $(k_1 - k_2)^2 dA$ is Möbius invariant.

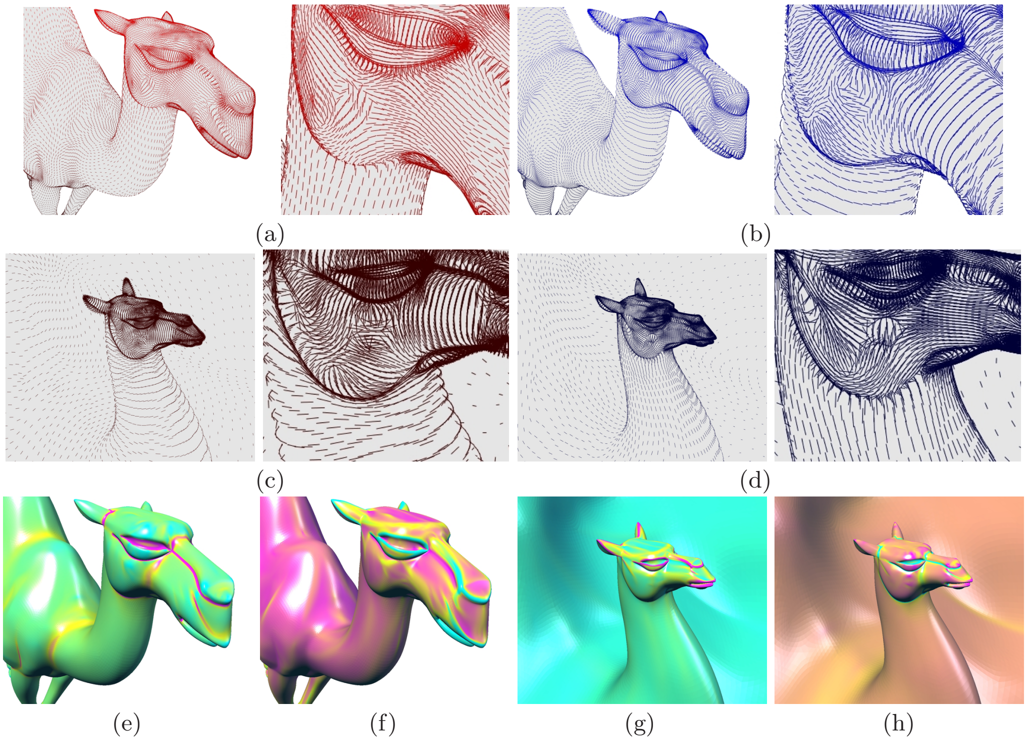

Figure 5. Duality of principal curvatures and their corresponding principal directions for the input mesh M (a,b,e,f) and its inversion $\tilde{M}$ (c,d,g,h). (a): $\mathbf{t}_1$. (b): $\mathbf{t}_2$. (c): $\tilde{\mathbf{t}}_1$. (d): $\tilde{\mathbf{t}}_2$. (e): k_1. (f): k_2. (g): $\tilde{k}_1$. (h): $\tilde{k}_2$. Here the input and its inversion ($c = 0.2$) meshes are shown in (a,b) and (c,d,e) of Fig. 1, respectively.

Differentiating the principal curvatures $\tilde{k}_1$ and $\tilde{k}_2$ of $\tilde{M}$ along their corresponding curvature lines yields (see Appendix B for detailed derivations)

$$\frac{c^2}{r^2}\tilde{e}_1 = -\frac{r^2}{c^2}e_2, \qquad \frac{c^2}{r^2}\tilde{e}_2 = -\frac{r^2}{c^2}e_1, \qquad d\tilde{s}_1 = \frac{c^2}{r^2}ds_2, \quad \text{and} \quad d\tilde{s}_2 = \frac{c^2}{r^2}ds_1 \tag{3.5}$$

where $\tilde{s}_1$ and $\tilde{s}_2$ are the arc-lengths of curvature lines of $\tilde{M}$ corresponding to $\tilde{k}_1$ and $\tilde{k}_2$, respectively. Note that the curvature lines of M are mapped onto the curvature lines of $\tilde{M}$ such that $\tilde{\mathbf{t}}_1 = \mathbf{t}_2$ and $\tilde{\mathbf{t}}_2 = \mathbf{t}_1$, where $\tilde{\mathbf{t}}_1$ and $\tilde{\mathbf{t}}_2$ are the principal directions corresponding to the principal curvatures $\tilde{k}_1$ and $\tilde{k}_2$, respectively, see Figs 5 and 6.

Therefore the measure (3.3) is Möbius invariant. Further, simple algebraic manipulations (addition, multiplication, division) with the above formulas yield Möbius invariance of

$$\frac{(e_1^2+e_2^2)dA}{(k_1-k_2)^2}, \qquad \frac{(e_1+e_2)^2dA}{(k_1-k_2)^2}, \qquad \frac{(e_1-e_2)^2dA}{(k_1-k_2)^2}, \qquad \frac{e_1e_2dA}{(k_1-k_2)^2}, \tag{3.6}$$

$$(k_1-k_2)^2dA, \qquad \text{and} \qquad \sqrt{e_1^2+e_2^2}\,dA. \tag{3.7}$$

In particular, integration over M of (3.7) gives

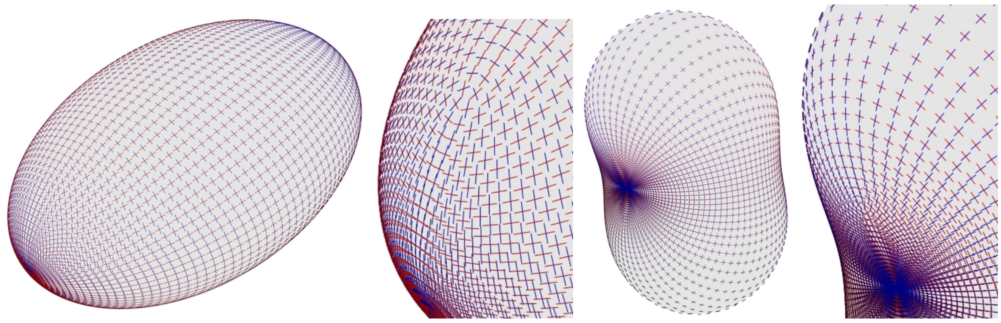

(a) (b)

FIGURE 6. Duality of principal directions. (a): Principal directions $\mathbf{t}_1$ and $\mathbf{t}_2$ of the input ellipsoid mesh shown in Fig. 4 (a). (b): Principal directions $\tilde{\mathbf{t}}_1$ and $\tilde{\mathbf{t}}_2$ of inversion of (a) where $c = 1.0$.

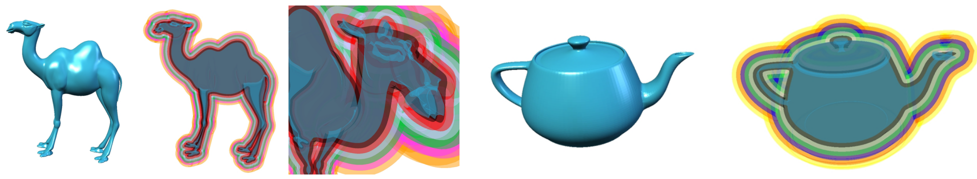

FIGURE 7. Normal offset examples.

$$\int_M (k_1 - k_2)^2 dA \qquad \text{and} \qquad \int_M \sqrt{e_1^2 + e_2^2} dA$$

which are the celebrated Willmore energy and a surface energy we call the will-even-more energy: a novel Möbius invariant extension for minimum variation surfaces (MVS) of (Moreton and Séquin 1992; Joshi and Séquin 2007), respectively. Möbius invariance of $(k_1 - k_2)^2 dA$ is also mentioned in (Blaschke 1929, §74).

3.1. *Normal offset invariance*

Consider a normal offset surface $\hat{M}$ of M such that $\hat{\boldsymbol{x}} = \boldsymbol{x} + \alpha \boldsymbol{n}$ of M where $\boldsymbol{n}$ is the unit normal of $\boldsymbol{x}$ and $\alpha \in \mathbb{R}$ is a constant, see Fig. 7 for some examples. Let $\hat{k}_1$ and $\hat{k}_2$ be the principal curvatures of $\hat{\boldsymbol{x}}$ where $\hat{k}_1 \geq \hat{k}_2$. According to (Hosaka 1992), we have

$$d\hat{A} = (1 - \alpha k_1)(1 - \alpha k_2) dA, \qquad d\hat{s}_1 = (1 - \alpha k_1) ds_1, \qquad d\hat{s}_2 = (1 - \alpha k_2) ds_2,$$

$$\hat{k}_1 = \frac{k_1}{1 - \alpha k_1}, \qquad \text{and} \qquad \hat{k}_2 = \frac{k_2}{1 - \alpha k_2}$$

where $\hat{s}_1$ and $\hat{s}_2$ are the arc-lengths of curvature lines of $\hat{M}$ corresponding to $\hat{k}_1$ and $\hat{k}_2$, respectively.

By using the principal coordinate system, we have

$$\hat{e}_1 = \frac{\partial}{\partial \tilde{s}_1} \frac{k_1}{1 - \alpha k_1} = \frac{\partial s_1}{\partial \tilde{s}_1} \frac{\partial}{\partial s_1} \frac{k_1}{1 - \alpha k_1} = \frac{e_1}{(1 - \alpha k_1)^3} \qquad \text{and} \qquad \hat{e}_2 = \frac{e_2}{(1 - \alpha k_2)^3}$$

where $\hat{e}_1$ and $\hat{e}_2$ are the derivatives of the principal curvatures $\hat{k}_1$ and $\hat{k}_2$ along their corresponding curvature lines, respectively.

Therefore the measure (3.3) and last quantity in (3.6) are offset invariant.

3.2. *Focal surfaces*

Consider the focal surfaces of M such that

$$\mathbf{f}_1 = \boldsymbol{x} + \frac{1}{k_1}\boldsymbol{n} \qquad \text{and} \qquad \mathbf{f}_2 = \boldsymbol{x} + \frac{1}{k_2}\boldsymbol{n}.$$

Thus

$$\frac{\partial \mathbf{f}_1}{\partial s_1} = \frac{\partial \boldsymbol{x}}{\partial s_1} - \frac{1}{k_1^2}\frac{\partial k_1}{\partial s_1}\boldsymbol{n} + \frac{1}{k_1}\boldsymbol{n}_{s_1} \qquad \text{and} \qquad \frac{\partial \mathbf{f}_2}{\partial s_2} = \frac{\partial \boldsymbol{x}}{\partial s_2} - \frac{1}{k_2^2}\frac{\partial k_2}{\partial s_2}\boldsymbol{n} + \frac{1}{k_2}\boldsymbol{n}_{s_2}.$$

By using the principal coordinate system, we have

$$\frac{\partial \mathbf{f}_1}{\partial s_1} = -\frac{e_1}{k_1^2}\boldsymbol{n}, \qquad \frac{\partial \mathbf{f}_2}{\partial s_2} = -\frac{e_2}{k_2^2}\boldsymbol{n}, \qquad \text{and} \qquad df_1 df_2 = \frac{|e_1||e_2|}{k_1^2 k_2^2} ds_1 ds_2$$

where $df_1 = |d\mathbf{f}_1|$ and $df_2 = |d\mathbf{f}_2|$. Therefore,

$$\frac{df_1 df_2}{(R_1 - R_2)^2} = \frac{|e_1||e_2| dA}{(k_1 - k_2)^2}.$$

Since the right hand side of the above equation is equivalent to (3.3) which is Möbius and normal offset invariant, the measure (3.1) is also Möbius and normal offset invariant.

3.3. *Dual properties*

Since $\mathbf{t}_1 = \tilde{\mathbf{t}}_2$ and $\mathbf{t}_2 = \tilde{\mathbf{t}}_1$, we have

$$|e_1| ds_1^2 = |\tilde{e}_2| d\tilde{s}_2^2, \qquad |e_1| dA = |\tilde{e}_2| d\tilde{A}, \qquad |e_2| ds_2^2 = |\tilde{e}_1| d\tilde{s}_1^2, \quad \text{and} \quad |e_2| dA = |\tilde{e}_1| d\tilde{A}.$$

Now (3.4), (3.5), and relations $ds_1 ds_2 = dA$ and $d\tilde{s}_1 d\tilde{s}_2 = d\tilde{A}$ imply that

$$\frac{(k_1 - k_2)^2}{(\tilde{k}_1 - \tilde{k}_2)^2} = \frac{|e_2|}{|\tilde{e}_1|} = \frac{|e_1|}{|\tilde{e}_2|} = \frac{c^4}{r^4} = \frac{d\tilde{A}}{dA} = \frac{d\tilde{s}_1 d\tilde{s}_2}{ds_1 ds_2} = \frac{d\tilde{s}_1^2}{ds_2^2} = \frac{d\tilde{s}_2^2}{ds_1^2}.$$

Therefore,

$$|e_1| ds_2^2 = |\tilde{e}_2| d\tilde{s}_1^2, \qquad |e_2| ds_1^2 = |\tilde{e}_1| d\tilde{s}_2^2,$$

$$\frac{|e_1|}{(k_1 - k_2)^2} = \frac{|\tilde{e}_2|}{(\tilde{k}_1 - \tilde{k}_2)^2}, \qquad \text{and} \qquad \frac{|e_2|}{(k_1 - k_2)^2} = \frac{|\tilde{e}_1|}{(\tilde{k}_1 - \tilde{k}_2)^2}.$$

Further, let $\tilde{\mathbf{n}}$ be the unit normal vector of $\tilde{\boldsymbol{x}}$, and then (3.2) implies that

$$\frac{ds_1 df_1}{R_1^2} = |\tilde{e}_2| d\tilde{s}_2^2 = \frac{d\tilde{s}_2 d\tilde{f}_2}{\tilde{R}_2^2} \qquad \text{and} \qquad \frac{ds_2 df_2}{R_2^2} = |\tilde{e}_1| d\tilde{s}_1^2 = \frac{d\tilde{s}_1 d\tilde{f}_1}{\tilde{R}_1^2}$$

where $\tilde{R}_1 = 1/\tilde{k}_1$, $\tilde{R}_2 = 1/\tilde{k}_2$, $d\tilde{f}_1 = |d\tilde{\mathbf{f}}_1|$, $d\tilde{f}_2 = |d\tilde{\mathbf{f}}_2|$, $\tilde{\mathbf{f}}_1 = \tilde{\boldsymbol{x}} + \tilde{R}_1 \tilde{\mathbf{n}}$, and $\tilde{\mathbf{f}}_2 = \tilde{\boldsymbol{x}} + \tilde{R}_2 \tilde{\mathbf{n}}$.

4. Curvature extremum curves

The surface creases are defined as zero-crossings of curvature extremalities e_1 and e_2. The maximum (η_1) and minimum (η_2) curvature extremum lines of M are characterized by

$$\eta_1 : e_1 = 0, \quad \frac{\partial e_1}{\partial \mathbf{t}_1} < 0 \qquad \text{and} \qquad \eta_2 : e_2 = 0, \quad \frac{\partial e_2}{\partial \mathbf{t}_2} > 0. \tag{4.1}$$

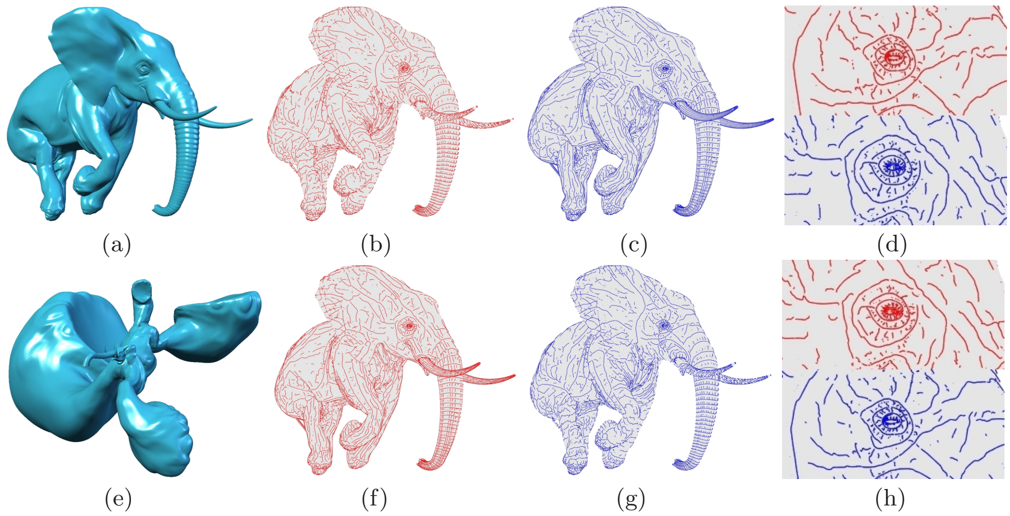

FIGURE 8. Extremum curves. (a): Input mesh M. (b): η_1 (maximum) of M. (c): η_2 (minimum) of M. (d): Zooms of (b,c). (e): $\tilde{M}$ which is an inversion of M where $c = 0.5$. (f): $\tilde{\eta}_1$ of $\tilde{M}$ mapped onto M. (g): $\tilde{\eta}_2$ of $\tilde{M}$ mapped onto M. (h): Zooms of (f,g).

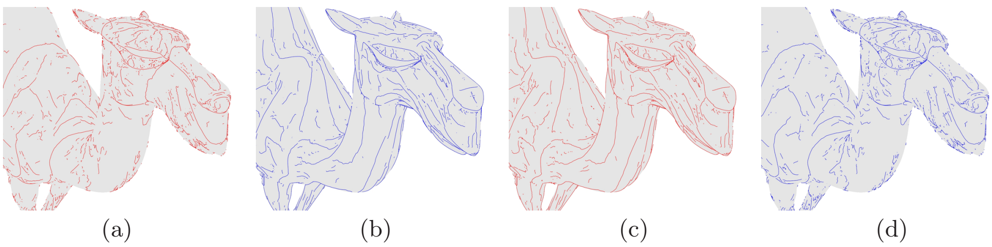

FIGURE 9. Extremum curves. Here the input mesh M and its inversion $\tilde{M}$ are shown in the images (a,b) and (c,d,e) of Fig. 1, respectively. (a): η_1 (maximum) of M. (b): η_2 (minimum) of M. (c): $\tilde{\eta}_1$ of $\tilde{M}$ mapped onto M. (d): $\tilde{\eta}_2$ of $\tilde{M}$ mapped onto M.

Also let us define the maximum ($\tilde{\eta}_1$) and minimum ($\tilde{\eta}_2$) curvature extremum lines of $\tilde{M}$ by

$$\tilde{\eta}_1 : \tilde{e}_1 = 0, \quad \frac{\partial \tilde{e}_1}{\partial \tilde{\mathbf{t}}_1} < 0 \qquad \text{and} \qquad \tilde{\eta}_2 : \tilde{e}_2 = 0, \quad \frac{\partial \tilde{e}_2}{\partial \tilde{\mathbf{t}}_2} > 0. \tag{4.2}$$

According to (3.5), a set of η_1 and η_2 is Möbius invariant. Unfortunately, their well-employed subsets called ridges and crest lines are not Möbius invariant, since their definitions include inequalities consist of principal curvatures. So it is interesting to investigate (4.1) and (4.2) as Möbius invariant surface creases.

According to (3.5) and by using the principal coordinate system, we have

$$\frac{\partial \tilde{e}_1}{\partial \tilde{\mathbf{t}}_1} = -\frac{r^2}{c^6}(4r^2(\mathbf{t}_2 \cdot \boldsymbol{x})e_2 + r^4\frac{\partial e_2}{\partial s_2}) \quad \text{and} \quad \frac{\partial \tilde{e}_2}{\partial \tilde{\mathbf{t}}_2} = -\frac{r^2}{c^6}(4r^2(\mathbf{t}_1 \cdot \boldsymbol{x})e_1 + r^4\frac{\partial e_1}{\partial s_1}).$$

Since $\tilde{e}_1 = 0$ on $\tilde{\eta}_1$ implies $e_2 = 0$ and $\tilde{e}_2 = 0$ on $\tilde{\eta}_2$ implies $e_1 = 0$, and therefore

$$\frac{\partial \tilde{e}_1}{\partial \tilde{\mathbf{t}}_1} = -\frac{r^6}{c^6}\frac{\partial e_2}{\partial s_2} < 0 \Rightarrow \frac{\partial e_2}{\partial \mathbf{t}_2} > 0 \quad \text{on} \quad \tilde{\eta}_1 \quad \text{and} \quad \frac{\partial \tilde{e}_2}{\partial \tilde{\mathbf{t}}_2} = -\frac{r^6}{c^6}\frac{\partial e_1}{\partial s_1} > 0 \Rightarrow \frac{\partial e_1}{\partial \mathbf{t}_1} < 0 \quad \text{on} \quad \tilde{\eta}_2.$$

It leads that η_1 and η_2 are mapped onto $\tilde{\eta}_2$ and $\tilde{\eta}_1$, respectively by $\tilde{M} = \pi(M)$.

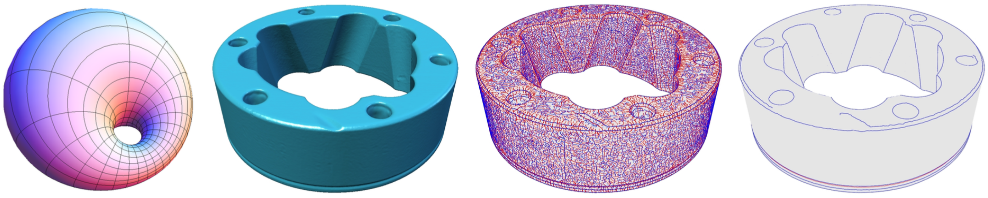

(a) (b) (c) (d)

FIGURE 10. Dupin's cyclide and filtering example. (a): A cyclide example. (b): Input scanned mechanical mesh M . (c): Curvature extremum curves η_1 and η_2 of M. (d): Filtered extremum curves of M via (4.3) where $T \geq 9.0$.

Figures 8 and 9 demonstrate dual sets of η_i and $\tilde{\eta}_i$, $i = 1, 2$ where remarkably similar patterns are obtained for η_1 and $\tilde{\eta}_2$ as well as η_2 and $\tilde{\eta}_1$. In our numerical experiments, M is orientated such that η_1 and η_2 correspond to the convex and concave shape features. The detected extremum lines include small surface features which are useful for some application such as surface quality evaluation. However more salient surface creases are preferable for other application, e.g. shape deformations by feature curves.

Let us consider the so-called Dupin's cyclides which are minimizers of the MVS and will-even-more (based on (3.7)) energies. The family of cyclides includes spheres, cylinders, cones, and tori, and they have been employed for several shape modeling tasks, see Foufou and Garnier (2004); Pottmann et al. (2008); Bo et al. (2011) for recent applications of the cyclides in geometric modeling as a CAGD primitive. The cyclides are characterized by $e_1 = 0 = e_2$. Thus, the cyclides do not have surface creases. Small perturbation of cyclides leads to surface creases and detecting salient subsets of extremum lines on a surface part close to cyclides is a difficult computational task.

Let ds and $d\tilde{s}$ be the arc-lengths of a curvature extremum line on M and $\tilde{M}$, respectively. The threshold proposed in (Yoshizawa et al. 2008)

$$T = \int \sqrt{|e_1| + |e_2|}ds = \int \sqrt{|\tilde{e}_1| + |\tilde{e}_2|}d\tilde{s} \tag{4.3}$$

is Möbius invariant. Since T also measures deviation from cyclides, (4.3) is useful to eliminate unessential extremum lines where T is smaller than a given threshold value. Figures 10-12 demonstrate how well our Möbius invariant thresholding scheme provides salient subsets of the curvature extremum lines.

5. Conclusion

We studied the invariance properties of curvature-based energies and demonstrated their application to salient crease detection on surface meshes. In addition, the principal curvature derivatives along their corresponding curvature lines were investigated in connection with the Möbius cross energy (2.1). It leads to (3.3) which is Möbius and normal offset invariant. Developing applications of (3.3) to CG and CAD is our future work. One possible application of (3.3) is character animation, since the Gauss's linking number employed in Ho and Komura (2009) is closely related to (2.1) (He 2002).

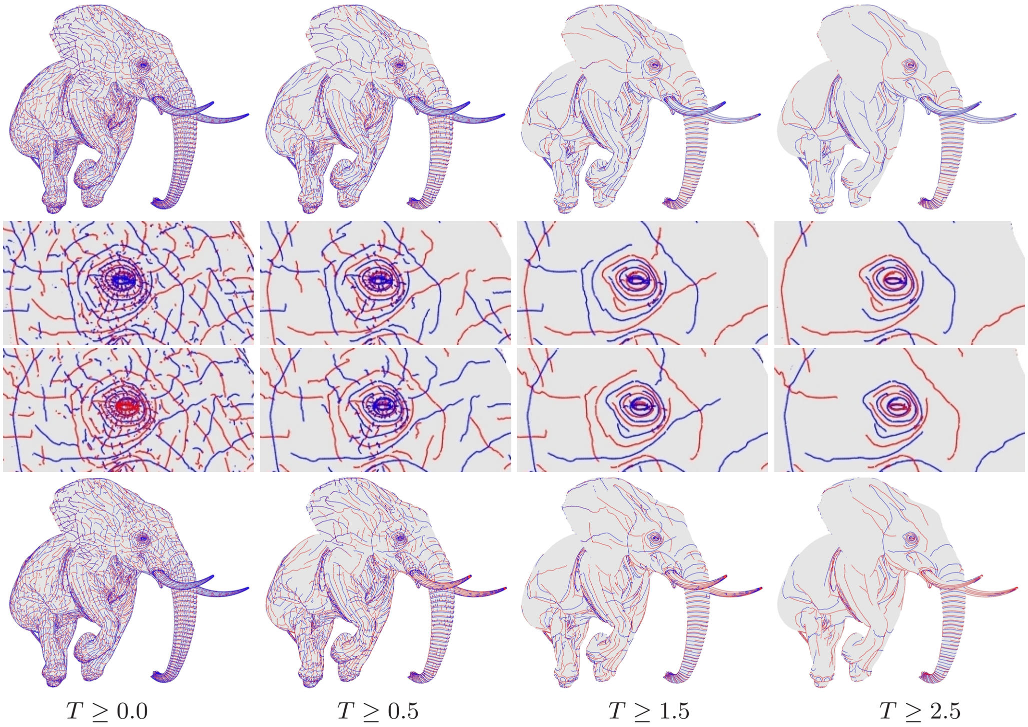

FIGURE 11. Filtering examples. Top and bottom images represent the filtered curvature extremum curves via (4.3) for the input mesh M (top, η_1 and η_2) and its inversion $\tilde{M}$ (bottom, $\tilde{\eta}_1$ and $\tilde{\eta}_2$) mapped onto M, respectively. Here the input and inversion meshes are shown in the images (a) and (e) of Fig. 8, respectively.

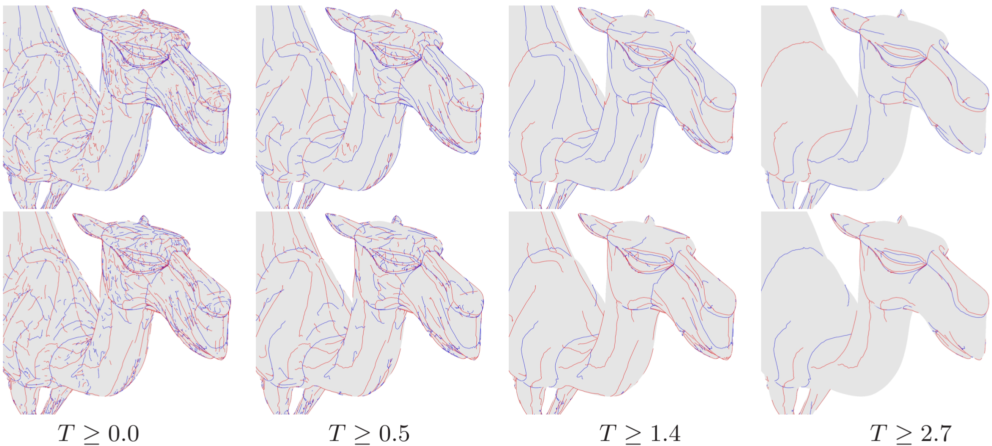

FIGURE 12. Filtering examples. Top and bottom images represent the filtered curvature extremum curves via (4.3) for the input mesh M (top, η_1 and η_2) and its inversion $\tilde{M}$ (bottom, $\tilde{\eta}_1$ and $\tilde{\eta}_2$) mapped onto M, respectively. Here the input and its inversion meshes are shown in the images (a,b) and (c,d,e) of Fig. 1, respectively.

Acknowledgements.

This work was supported in part by Grants-in-Aid for Scientific Research of Japan (24700182). The models are courtesy of AIM@SHAPE shape repository (Camel, Rolling Stage, and Teapot) and MIT Computer Graphics Group (Elephant).

REFERENCES

Blair, D. E., 2000. Inversion Theory and Conformal Mapping. AMS.

Blaschke, W., 1929. Differentialgeometrie und Geometrische Grundlagen von Einsteins Relativitätstheorie III: Differentialgeometrie der Kreise und Kugeln. Springer, Berlin.

Bo, P., Pottmann, H., Kilian, M., Wang, W., Wallner, J., 2011. Circular arc structures. ACM Transaction on Graphics 30 (4), 101:1–101:12, proc. of ACM SIGGRAPH.

Foufou, S., Garnier, L., 2004. Dupin cyclide blends between quadric surfaces for shape modeling. Computer Graphics Forum 23 (3), 321–330, proc. of Eurographics.

Freedman, M. H., He, Z.-X., Wang, Z.-H., 1994. Möbius energy of knots and unknots. Annals of Mathematics 139 (1), 1–50.

He, Z.-X., 2002. On the minimizers of the möbius cross energy of links. Experimental Mathematics 11 (2), 243–248.

Ho, E. S. L., Komura, T., 2009. Character motion synthesis by topology coordinates. Computer Graphics Forum 28 (2), 299–308, proc. of EUROGRAPHICS.

Hosaka, M., 1992. Modeling of Curves and Surfaces in CAD/CAM. Springer, Berlin.

Joshi, P., Séquin, C., 2007. Energy minimizers for curvature-based surface functionals. Computer-Aided Design and Applications 4 (5), 607–618.

Moreton, H. P., Séquin, C. H., 1992. Functional optimization for fair surface design. In: Proceedings of ACM SIGGRAPH. pp. 167–176.

O'Hara, J., 2003. Energy of Knots and Conformal Geometry. World Scientific Publishing.

Pottmann, H., Schiftner, A., Bo, P., Schmiedhofer, H., Wang, W., Baldassini, N., Wallner, J., 2008. Freeform surfaces from single curved panels. ACM Transaction on Graphics 27 (3), 76:1–76:10, proc. of ACM SIGGRAPH.

Struik, D. J., 1988. Lectures on Classical Differential Geometry: Second Edition. Dover Publications, Inc. New York.

Weatherburn, C. E., 1927. Differential Geometry of Three Dimensions, volume I. Cambridge University Press.

Yoshizawa, S., Belyaev, A., Yokota, H., Seidel, H.-P., 2008. Fast, robust, and faithful methods for detecting crest lines on meshes. Computer Aided Geometric Design 25 (8), 545–560.

Appendix A: Curvatures of $\tilde{\boldsymbol{x}}$.

For a given surface $\boldsymbol{x} = \boldsymbol{x}(u, v)$, consider a parametric representation of spherical inversion with its radius c: $\tilde{\boldsymbol{x}} = \tilde{\boldsymbol{x}}(u, v) = \frac{c^2}{r^2(u,v)}\boldsymbol{x}(u, v)$ where $r^2 = r^2(u, v) = \boldsymbol{x} \cdot \boldsymbol{x}$. Since $\frac{\partial(\boldsymbol{x}\cdot\boldsymbol{x})}{\partial u} = 2\boldsymbol{x}_u \cdot \boldsymbol{x} = 2\frac{\partial r}{\partial u}r = 2r_u r$ and $\frac{\partial(\boldsymbol{x}\cdot\boldsymbol{x})}{\partial v} = 2\boldsymbol{x}_v \cdot \boldsymbol{x} = 2\frac{\partial r}{\partial v}r = 2r_v r$, we have $r_u = \frac{\boldsymbol{x}_u\cdot\boldsymbol{x}}{r}$ and $r_v = \frac{\boldsymbol{x}_v\cdot\boldsymbol{x}}{r}$, and then the basic tangents of $\tilde{\boldsymbol{x}}$ are given by differentiating $\tilde{\boldsymbol{x}}$ w.r.t. u and v:

$$\frac{\partial\tilde{\boldsymbol{x}}}{\partial u} = \tilde{\boldsymbol{x}}_u = -2\frac{c^2}{r^4}(\boldsymbol{x}_u \cdot \boldsymbol{x})\boldsymbol{x} + \frac{c^2}{r^2}\boldsymbol{x}_u, \tag{A.1}$$

$$\frac{\partial\tilde{\boldsymbol{x}}}{\partial v} = \tilde{\boldsymbol{x}}_v = -2\frac{c^2}{r^4}(\boldsymbol{x}_v \cdot \boldsymbol{x})\boldsymbol{x} + \frac{c^2}{r^2}\boldsymbol{x}_v \tag{A.2}$$

where $\boldsymbol{x}_u = \frac{\partial\boldsymbol{x}}{\partial u}$ and $\boldsymbol{x}_v = \frac{\partial\boldsymbol{x}}{\partial v}$ are the basic tangents of $\boldsymbol{x}$. Then, their inner products give us the coefficients of the first fundamental form of $\tilde{\boldsymbol{x}}$:

$$\tilde{E} = \tilde{\boldsymbol{x}}_u^2 = \frac{c^4}{r^4}E, \quad \tilde{F} = \tilde{\boldsymbol{x}}_u \cdot \tilde{\boldsymbol{x}}_v = \frac{c^4}{r^4}F, \quad \tilde{G} = \tilde{\boldsymbol{x}}_v^2 = \frac{c^4}{r^4}G,$$

where $E = \boldsymbol{x}_u^2$, $F = \boldsymbol{x}_u \cdot \boldsymbol{x}_v$, and $G = \boldsymbol{x}_v^2$ are the coefficients of the first fundamental form of $\boldsymbol{x}$. Thus, the area element of $\tilde{\boldsymbol{x}}$ is given by

$$\iint d\tilde{A} = \iint \sqrt{\tilde{E}\tilde{G} - \tilde{F}^2}\, dudv = \iint \frac{c^4}{r^4}dA,$$

where $dA = \sqrt{EG - F^2}\, dudv$ is the area element of $\boldsymbol{x}$.

Let $\boldsymbol{n}$ be the unit normal vector of $\boldsymbol{x}$. The unit normal vector of $\tilde{\boldsymbol{x}}$ is given by

$$\tilde{\mathbf{n}} = \frac{\tilde{\boldsymbol{x}}_u \times \tilde{\boldsymbol{x}}_v}{\sqrt{\tilde{E}\tilde{G} - \tilde{F}^2}} = -\frac{2}{r^2}((\boldsymbol{x}_v \cdot \boldsymbol{x})\boldsymbol{x}_u - (\boldsymbol{x}_u \cdot \boldsymbol{x})\boldsymbol{x}_v) \times \boldsymbol{x} + \boldsymbol{n},$$

By using the formulas of vector triple product:

$$\mathbf{a} \times (\mathbf{b} \times \mathbf{c}) = (\mathbf{a} \cdot \mathbf{c})\mathbf{b} - (\mathbf{a} \cdot \mathbf{b})\mathbf{c}, (\mathbf{a} \times \mathbf{b}) \times \mathbf{c} = (\mathbf{c} \cdot \mathbf{a})\mathbf{b} - (\mathbf{c} \cdot \mathbf{b})\mathbf{a},$$

we obtain

$$\tilde{\mathbf{n}} = -\frac{2}{r^2}(\boldsymbol{x} \times \boldsymbol{n}) \times \boldsymbol{x} + \boldsymbol{n} = \frac{2}{r^2}(\boldsymbol{x} \cdot \boldsymbol{n})\boldsymbol{x} - \boldsymbol{n}.$$

Differentiating (A.1) and (A.2), and their inner products with $\tilde{\mathbf{n}}$ lead to the coefficients of the second fundamental form of $\tilde{\boldsymbol{x}}$:

$$\begin{aligned}
\tilde{L} = \tilde{\boldsymbol{x}}_{uu} \cdot \tilde{\mathbf{n}} &= (8\frac{c^2}{r^6}(\boldsymbol{x}_u \cdot \boldsymbol{x})^2\boldsymbol{x} - 2\frac{c^2}{r^4}(\boldsymbol{x}_{uu} \cdot \boldsymbol{x} + E)\boldsymbol{x} + \\
&\quad -4\frac{c^2}{r^4}(\boldsymbol{x}_u \cdot \boldsymbol{x})\boldsymbol{x}_u + \frac{c^2}{r^2}\boldsymbol{x}_{uu}) \cdot (\frac{2}{r^2}(\boldsymbol{x} \cdot \boldsymbol{n})\boldsymbol{x} - \boldsymbol{n}) \\
&= -\frac{c^2}{r^2}(L + \frac{2}{r^2}(\boldsymbol{x} \cdot \boldsymbol{n})E),
\end{aligned}$$

and similar computations give us

$$\tilde{M} = \tilde{\boldsymbol{x}}_{uv} \cdot \tilde{\mathbf{n}} = -\frac{c^2}{r^2}(M + \frac{2}{r^2}(\boldsymbol{x} \cdot \boldsymbol{n})F), \qquad \tilde{N} = \tilde{\boldsymbol{x}}_{vv} \cdot \tilde{\mathbf{n}} = -\frac{c^2}{r^2}(N + \frac{2}{r^2}(\boldsymbol{x} \cdot \boldsymbol{n})G),$$

where $L = \boldsymbol{x}_{uu} \cdot \boldsymbol{n}$, $M = \boldsymbol{x}_{uv} \cdot \boldsymbol{n}$, and $N = \boldsymbol{x}_{vv} \cdot \boldsymbol{n}$ are the coefficients of the second fundamental form of $\boldsymbol{x}$.

Substituting the above results into the following formulas of the mean and Gaussian curvatures provides

$$\begin{aligned}
\tilde{H} &= \frac{1}{2}\frac{\tilde{E}\tilde{N} - 2\tilde{F}\tilde{M} + \tilde{G}\tilde{L}}{\tilde{E}\tilde{G} - \tilde{F}^2} = -\frac{r^2}{c^2}H - 2\frac{(\boldsymbol{x} \cdot \boldsymbol{n})}{c^2}, \\
\tilde{K} &= \frac{\tilde{L}\tilde{N} - \tilde{M}^2}{\tilde{E}\tilde{G} - \tilde{F}^2} = \frac{r^4}{c^4}K + 4\frac{r^2}{c^4}(\boldsymbol{x} \cdot \boldsymbol{n})H + 4\frac{(\boldsymbol{x} \cdot \boldsymbol{n})^2}{c^4}
\end{aligned}$$

where $H = \frac{1}{2}\frac{EN-2FM+GL}{EG-F^2}$ and $K = \frac{LN-M^2}{EG-F^2}$ are the mean and Gaussian curvatures of $\boldsymbol{x}$, respectively. Let $\tilde{k}_1$ and $\tilde{k}_2$ be the principal curvatures of $\tilde{\boldsymbol{x}}$ then, substituting the above equations to $\tilde{H} = (\tilde{k}_1 + \tilde{k}_2)/2$, $\tilde{K} = \tilde{k}_1\tilde{k}_2$, $\tilde{k}_1 = \tilde{H} + \sqrt{\tilde{H}^2 - \tilde{K}}$, and $\tilde{k}_2 = \tilde{H} - \sqrt{\tilde{H}^2 - \tilde{K}}$ with $k_1 \geq k_2$, $c^2 > 0$, and $r^2 \geq 0$ gives

$$\tilde{k}_1 = -\frac{r^2}{c^2}k_2 - 2\frac{(\boldsymbol{x} \cdot \boldsymbol{n})}{c^2}, \qquad \tilde{k}_2 = -\frac{r^2}{c^2}k_1 - 2\frac{(\boldsymbol{x} \cdot \boldsymbol{n})}{c^2}$$

where k_1 and k_2 are the principal curvatures of $\boldsymbol{x}$.

Appendix B: Curvature derivatives of $\tilde{\boldsymbol{x}}$.

Differentiating $\tilde{k}_1$ and $\tilde{k}_2$ in (3.4) w.r.t. the parameters v and u, respectively, gives

$$\begin{aligned}
\frac{\partial \tilde{k}_1}{\partial v} &= -2\frac{r}{c^2}\frac{\boldsymbol{x}_v \cdot \boldsymbol{x}}{r}k_2 - \frac{r^2}{c^2}\frac{\partial k_2}{\partial v} - 2\frac{\boldsymbol{x}_v \cdot \boldsymbol{n} + \boldsymbol{x} \cdot \boldsymbol{n}_v}{c^2}, \\
\frac{\partial \tilde{k}_2}{\partial u} &= -2\frac{r}{c^2}\frac{\boldsymbol{x}_u \cdot \boldsymbol{x}}{r}k_1 - \frac{r^2}{c^2}\frac{\partial k_1}{\partial u} - 2\frac{\boldsymbol{x}_u \cdot \boldsymbol{n} + \boldsymbol{x} \cdot \boldsymbol{n}_u}{c^2}.
\end{aligned}$$

In a small vicinity of non-umbilical point P of $\boldsymbol{x}$, let us consider the lines of curvature parameterized by their arc-lengths. Then the surface is locally represented in parametric form $\boldsymbol{x} = \boldsymbol{x}(u,v)$ for which

$$\boldsymbol{x}_u = \mathbf{t}_1, \qquad \boldsymbol{x}_v = \mathbf{t}_2,$$

and the Rodrigues'curvature formula (Struik 1988, p. 94) gives

$$\boldsymbol{n}_u = -k_1\mathbf{t}_1, \qquad \boldsymbol{n}_v = -k_2\mathbf{t}_2.$$

Now differentiating $\tilde{k}_1$ and $\tilde{k}_2$ in (3.4) along the *non*-corresponding curvature lines of $\boldsymbol{x}$ gives

$$\frac{\partial \tilde{k}_1}{\partial v} = \frac{\partial \tilde{k}_1}{\partial \mathbf{t}_2} = -2\frac{r}{c^2}\frac{\mathbf{t}_2 \cdot \boldsymbol{x}}{r}k_2 - \frac{r^2}{c^2}e_2 - 2\frac{\mathbf{t}_2 \cdot \boldsymbol{n} - k_2\mathbf{t}_2 \cdot \boldsymbol{x}}{c^2} = -\frac{r^2}{c^2}e_2,$$

where $\mathbf{t}_2 \cdot \boldsymbol{n} = 0$ (because the principal directions live in the tangent plane of $\boldsymbol{x}$) and similar computations give us $\frac{\partial \tilde{k}_2}{\partial u}$:

$$\frac{\partial \tilde{k}_1}{\partial v} = -\frac{r^2}{c^2}e_2, \qquad \frac{\partial \tilde{k}_2}{\partial u} = -\frac{r^2}{c^2}e_1. \tag{B.1}$$

Now let us denote by $\tilde{u}$ and $\tilde{v}$ the arc-length parameterizations of the $\tilde{k}_1$ and $\tilde{k}_2$ curvature lines of $\tilde{\boldsymbol{x}}$, respectively, in a small vicinity of point $\tilde{P} \in \tilde{\boldsymbol{x}}$, the inversion image of $P \in \boldsymbol{x}$. Then, according to $|d\tilde{\boldsymbol{x}}| = (c^2/r^2)|d\boldsymbol{x}|$, we have

$$d\tilde{u} = c^2 dv/r^2, \qquad d\tilde{v} = c^2 du/r^2. \tag{B.2}$$

In view of (B.1) and (B.2), we have

$$\frac{\partial \tilde{k}_1}{\partial \tilde{\mathbf{t}}_1} = \frac{\partial \tilde{k}_1}{\partial \tilde{u}} = \frac{\partial v}{\partial \tilde{u}}\frac{\partial \tilde{k}_1}{\partial v} = \frac{r^2}{c^2}(-\frac{r^2}{c^2}e_2), \qquad \frac{\partial \tilde{k}_2}{\partial \tilde{\mathbf{t}}_2} = \frac{\partial \tilde{k}_2}{\partial \tilde{v}} = \frac{\partial u}{\partial \tilde{v}}\frac{\partial \tilde{k}_2}{\partial u} = \frac{r^2}{c^2}(-\frac{r^2}{c^2}e_1).$$

Consequently, the curvature derivatives $\tilde{e}_1 = \partial\tilde{k}_1/\partial\tilde{\mathbf{t}}_1$ and $\tilde{e}_2 = \partial\tilde{k}_2/\partial\tilde{\mathbf{t}}_2$ relate to e_1 and e_2 by the following equations:

$$\frac{c^2}{r^2}\tilde{e}_1 = -\frac{r^2}{c^2}e_2, \qquad \frac{c^2}{r^2}\tilde{e}_2 = -\frac{r^2}{c^2}e_1.$$